JOURNAL OF AGRICULTURAL AND FOOD CHEMISTRY

Reaction Mechanisms in Delignification of Pine Kraft-AQ Pulp with Hydrogen Peroxide Using Mn(IV)-Me$_4$DTNE as Catalyst

CHEN-LOUNG CHEN,*,† EWELLYN A. CAPANEMA,† AND HANNA S. GRACZ‡

Department of Wood and Paper Science, North Carolina State University, Raleigh, North Carolina 27695-8005, and Department of Biochemistry, North Carolina State University, Raleigh, North Carolina 27695-7622

Pine Kraft-AQ pulp was bleached with hydrogen peroxide catalyzed by [LMn(IV)$_2$ (μ-O)$_3$](ClO$_4$)$_2$ at 80 °C for 120 min under optimum reaction conditions. The resulting bleached pulp was hydrolyzed with cellulase to obtain insoluble and soluble residual lignins. The alkaline effluent from the bleaching was acidified to precipitate alkaline soluble lignin. These lignin preparations were purified, and then analyzed by 2D HMQC NMR spectroscopic techniques. The results showed that biphenyl (5−5) and stilbene structures are preferentially degraded in the bleaching process, while β-*O*-4, β-5, and $\beta-\beta$ structures undergo degradation only to a lesser extent. This implies that hydrogen peroxide bleaching using the catalyst is more effective in delignification of softwood pulps than hardwood pulps. The possible reaction mechanisms for the delignification of residual lignin in the pine Kraft-AQ pulp in the bleaching process are discussed on the basis of the 2D HMQC NMR spectroscopic data and the model compound experiments.

KEYWORDS: Pine Kraft-AQ pulp; binucleus Mn(IV) complex; hydrogen peroxide bleaching; catalysis; residual lignins; alkaline soluble lignin; 2D HMQC NMR spectroscopic technique; epoxidation of conjugated double bonds

INTRODUCTION

It is well established that hydrogen peroxide becomes effective as a delignifying agent only at temperatures above 100 °C (*1*, *2*). However, Odermatt et al. (*3*) and Cui et al. (*4*−*6*) showed that upon addition of a binucleus manganese complex [LMn(IV)(μ-O)$_3$Mn(IV)] (ClO$_4$)$_2$ (**C-2**) (**Figure 1**), where L is 1,2-bis(4,7-dimethyl-1,4,7-triazacyclonon-1-yl)ethane (Me$_4$-DTNE), at relatively low temperatures (30−80 °C), hydrogen peroxide easily oxidizes nonphenolic lignin model compounds such as those with α-hydroxyl and conjugated double bonds that otherwise would not be oxidized by hydrogen peroxide. Kinetics studies on pulp delignification using hydrogen peroxide catalyzed by **C-2** showed that selectivity and reactivity of hydrogen peroxide as an oxidant is improved by the catalytic effect of **C-2**. Odermatt et al. (*3*) postulated that a similar binucleus manganese complex, [L$_1$Mn(IV)(μ-O)$_3$Mn(IV)L$_1$] (PF$_6$)$_2$] (**C-1**), where L$_1$ is 1,4,7-trimethyl-1,4,7-triazacyclononane (Me$_3$TACN), is less effective as a catalyst than **C-2** for the bleaching of pulps with hydrogen peroxide on the basis of a literature review and experimental data.

The catalyst **C-2** significantly increases the degree of delignification and the brightness, but decreases the viscosity slightly. The increase in the reaction temperature slightly increases the degree of delignification in the catalytic process, but does not appreciably affect the brightness. In the absence of a catalyst, hydrogen peroxide has a much higher capability to act as a nucleophile that attacks double bonds and carbonyl groups, leading to degradation of the chromophoric groups (*7*, *8*). The considerable increases in the degree of delignification and brightness improvement achieved by addition of the catalyst **C-2** shows that the catalysis improves hydrogen peroxide not only as an oxidant but also its reactivity as a nucleophile. Model compound experiments have established that **C-2** catalyzes the oxidation of α-hydroxyl groups to the corresponding α-carbonyl groups as well as epoxidation of double bonds conjugated to aromatic rings including stilbene type structures (**4**). The resulting epoxide intermediates then undergo anti-Markovnikov addition of hydroperoxide anions (HOO$^-$) under the reaction conditions leading to oxidative cleavage of the double bonds. Conceivably, these reactions contribute appreciably to improving

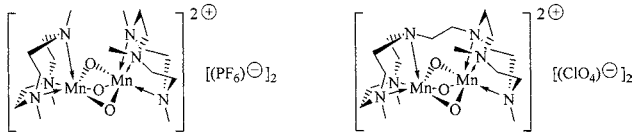

[L$_2$Mn(IV)$_2$(μ-O)$_3$](ClO$_4$)$_2$ (**C-1**)
[Mn(IV)-Me$_3$TACN]

L = 1.4,7-trimethyl-1,4,7-triazacyclononane

[LMn(IV)$_2$(μ-O)$_3$](ClO$_4$)$_2$ (**C-2**)
[Mn(IV)-Me$_4$DTNE]

L = 1,2-bis-(4,7-dimethyl-1,4,7-triazacyclonon-1-yl)ethane

Figure 1. Structures of binucleus manganese (IV) complexes.

* To whom correspondence should be addressed: E-mail: chen-loung_chen @ncsu.edu.
† Department of Wood and Paper Science.
‡ Department of Biochemistry.

10.1021/jf020992n CCC: $25.00
Published on Web 02/22/2003

the delignification of residual lignins in pulps. The objective of the present studies was, therefore, to elucidate the reaction mechanisms in the **C-2** catalyzed bleaching with hydrogen peroxide by observing the structural changes occurred in the residual lignin of pine Kraft-AQ pulp in the bleaching process using advanced ^{1}H-^{13}C correlation 2D-NMR spectroscopic techniques, such as the heteronuclear multiple-quantum coherence (HMQC) sequence. In addition, the change in the molecular mass distribution pattern of the residual lignin preparation was studied because radical species, such as hydroxyl radicals, could be involved in the bleaching process. This could lead to dehydrogenative polymerization of phenolic lignin fragments.

MATERIALS AND METHODS

The Kraft-AQ southern pine pulp with Kappa number 26.5 was provided by Covington mill of Westvaco Corporation. Degussa AG, Hanau, Germany, supplied the catalysts used in this study.

Delignification of Pine Kraft-AQ Pulp with Hydrogen Peroxide Catalyzed by Mn(IV)-Me_4DTNE (C-2). Kraft-AQ pulp (10 g, oven dried) with pulp consistency of 3% in deionized water was placed in a plastic bag. The pH of the pulp slurry was adjusted to 2.0 by concentrated H_2SO_4, and was immersed in a constant temperature water bath at 70 °C for 30 min. The pulp was removed from the bath, filtered, washed thoroughly with deionized water, and then oven dried. The Kappa number of the acid-washed pulp was 26.5. To a mixture of pulp (6 g, oven dried), and 0.12 g of NaOH (2% on oven dried pulp) and 50 mL of deionized water in a 200 mL Erlenmeyer flask on a constant temperature water bath was added 0.24 g of H_2O_2 (4% on oven dried pulp) and 0.45 mL of 0.04 mg/mL Mn(IV)-Me_4DTNE (**C-2**) solution (10 ppm on oven dried pulp). An appropriate amount of deionized water was then added to the resulting mixture to bring the pulp consistency of 10% under vigorous mechanical stirring and the reaction temperature was kept at 80 °C for 120 min with starting pH 11.5 and ending pH 10.9. The concentration of H_2O_2 after bleaching was determined and it was found that H_2O_2 was almost fully consumed. The kappa number, viscosity, and GE brightness were measured according to Tappi standard T236, T230, and T452 (*9*), respectively.

Isolation and Purification of Residual Lignin and Purification of Dissolved Lignins. The residual lignins were isolated from the unbleached and bleached Pine Kraft-AQ pulps by treatment with cellulase in acetate buffer solution (pH 4.5) according to the procedure of Chang and co-workers (*9*) to obtain the residual lignin from the pine Kraft-AQ pulp (KRL), and the insoluble residual lignin (ISRL-B) from the bleached pulp, respectively. A part of the residual lignins in the bleached pulp was dissolved in the cellulase solution (pH 4.5) and was recovered by acidification with 1 M H_2SO_4 solution to obtain the soluble residual lignin (SRL-B) from the bleached pulp. The lignin in the alkaline bleaching effluents was precipitated by acidifying the effluent with 1 M H_2SO_4 solution to obtain the alkaline soluble lignin (ASL). The resulting lignin preparations were purified according to the procedure described by Chang and co-workers (*10*). The yield of ISRL-B and SRL-B was 15.1 and 45.6% per residual lignin in the Kraft-AQ pulp. Elemental analysis: ISRL-B (C% 50.01, H% 5.46, N% not detectable); SRL-B (C% 55.96, H% 6.36, N% 3.84). The SRL-B contained ca. 23.8% of proteins as contaminants based on N% of the elemental analytical data: protein content (= 6.25 × N%).

Gel Permeation Chromatography. Gel permeation chromatography was performed on a Pharmacia FPLC system equipped with a 30 × 1 cm i.d. Superdex-75 column. A lignin sample (5 mg) was dissolved in 5 mL of 0.1 M NaOH solution containing 0.5 M LiCl. The sample solution was injected onto the column and eluted with 0.1 M NaOH solution containing 0.5 M LiCl with a flow rate of 0.3 mL/min. The eluent was monitored with a UV detector at 280 nm.

^{1}H-^{13}C Correlation 2D-NMR Spectroscopy. The NMR spectra were recorded with a Bruker AVANCE 500 MHz spectrometer with the Oxford narrow bore magnet after dissolving approximately 40 mg of each lignin preparation in 0.75 mL of DMSO-d_6 containing 0.01% TMS as internal standard. The system was controlled by the SGI INDY host workstation and the data were processed using the XWINNMR software. All measurements were carried out with a 5 mm i.d. ^{1}H/BB (^{109}Ag-^{31}P) triple-axis gradient probe (Nalorac Cryogenic Corp.). The operational frequency for the ^{1}H nucleus was 500.128 MHz and conditions for analysis included a temperature of 300 °K, a 90° pulse width of 10 μs, and a 1.5 s pulse delay (d_1).

Table 1. Physical Characteristics of the Bleached Pulps Obtained from the Noncatalyzed and Mn(IV)-ME_4DTNE (C-2)-Catalyzed Delignification of Pine Kraft-AQ Pulps with Hydrogen Peroxide at 60° and 80 °C for 120 min[a]

	delignification			
pulp samples	Kappa no.	degree of delig. (%)[c]	viscosity (mPa/s)	GE brightness
original pulp[b]	26.5		21.3	25.8
uncat. delig. (60 °C)	19.8	25.3	17.3	30.1
uncat. delig. (80 °C)	19.6	26.0	16.8	36.2
C-2-cat. delig. (60 °C)	16.4	38.1	15.2	40.3
C-2-cat. delig. (80 °C)	15.1	43.0	14.9	43.1

[a] Reaction conditions: see experimental section. [b] Acid-washed pulp. [c] Based on Kappa number of the acid-washed pulp.

RESULTS AND DISCUSSION

C-2-Catalyzed Delignification of Pine Kraft-AQ Pulp with Hydrogen Peroxide. The results of the pulp delignification show (**Table 1**) that in noncatalyzed delignification, only approximately 26% of the residual lignin can be removed. The lignin removal is accompanied by a slight loss in the viscosity and increase in the brightness. An increase in the reaction temperature from 60 to 80 °C does not affect appreciably the degree of delignification in the absence of the catalyst, but results in an additional loss in the viscosity and increase in the brightness. In addition, the optimum catalyst charge was determined in the previous investigation as 10 ppm on pulp (*3*), i.e., 6 times lower than the value reported in the earlier study (*6*).

Yields and Constituents of the Lignin Preparations Obtained from Bleached Pine Kraft-AQ Pulps. The total yield of lignin preparations isolated by the cellulase hydrolysis of the bleached pine Kraft-AQ pulp (Kappa number 15.1) was approximately 61%. The yield of the insoluble residual lignin (ISRL-B) and soluble residual lignin (SRL-B) was 15.1 and 45.5% of residual lignin in the bleached pulp, respectively. Although the yield of the SRL-B was much higher that that of the ISRL-B, the nitrogen content in the latter was below the detection limit while that in the former was 3.81%. Accordingly, the contribution of protein contaminants to the yield of SRL-B is 10.8% [= 6.25 × 0.0381(N%) × 45.5]. This was verified by the 2D HMQC spectrum, which will be discussed later. Consequently, the true yield of the SRL-B was 34.7% (= 45.5%−10.8%). The yield of alkaline soluble lignin (ASL) from the bleaching effluent was 22.3% of the residual lignin in the unbleached pine Kraft AQ pulp (Kappa number of 26.5). The nitrogen content in the ASL was also below the detection limit. Thus, approximately 72.1% of the residual lignin in the unbleached pine Kraft AQ pulp was recovered as lignin preparations after the bleaching. The fate of the remaining 28.9% of the residual lignin in the unbleached pulp is not known. However, it is likely that it consists mostly of volatile degradation products, which escaped from the reaction mixture during the processes of bleaching and isolation.

Structures Identified in the Pine Kraft-AQ Residual Lignin (KRL). The residual lignin (KRL) from the unbleached pine Kraft-AQ pulp was characterized by the 2D ^{1}H-^{13}C HMQC NMR technique. The oxygenated aliphatic region of the HMQC

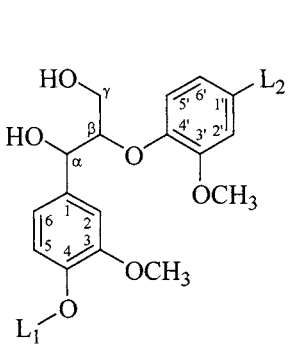

1, β-Aryl ether Structure (β-*O*-4)

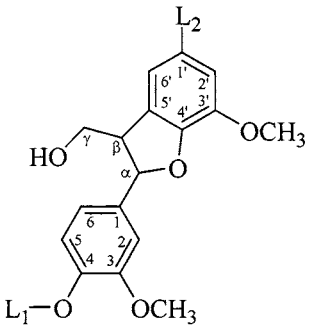

2, Phenylcoumaran Structure (β-5)

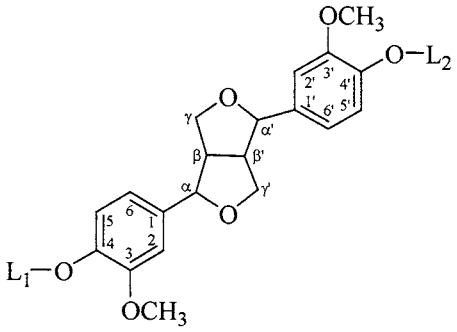

3, Pinoresinol Structure (β-β)

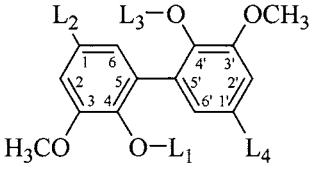

4, Biphenyl Structure (5-5)
7, L_2 = COR or COOH

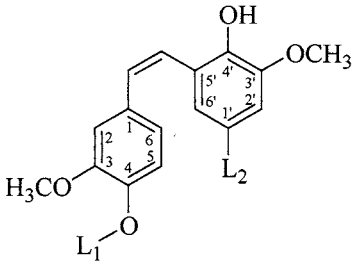

5, Stilbene Structure

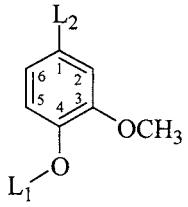

6, L_2 = COR or COOH

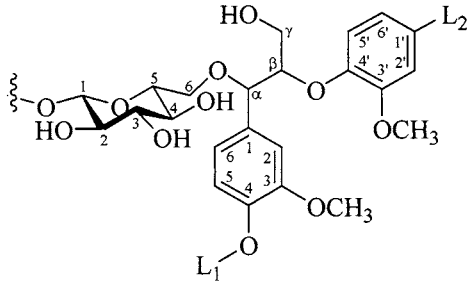

8, β-*O*-4 Structure with a Benzyl Ether Bond between C-α and C-6 of Glucose, a Type of LCC

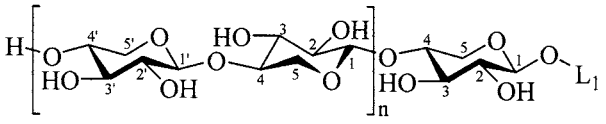

9, Xylan Backbone of Lignin-Carbohydrate Complexes (LCC), a Type of LCC

Figure 2. Major substructures in residual lignin preparations isolated from unbleached and bleached pine Kraft-AQ pulps and beaching effluent. L_1 = H or lignin moiety; L_2, L_3, and L_4 = lignin moieties.

spectrum of KRL (**Figure 3**A) shows clearly that the KRL contains arylglycerol-*β*-guaiacyl ether structures (*β*-*O*-4) (**1**), phenylcoumaran (*β*-5) (**2**), and pinoresinol (*β*−*β*) (**3**) structures (**Figure 2**). The presence of **1** is evidenced by the cross-signals at δ_C/δ_H 71.8/4.76, 84.6/4.28, and 60.2/3.56, corresponding to CH-α, CH-*β*, and CH-*γ* of **1**, respectively (*11*, *12*). The cross-signals at δ_C/δ_H 87.4/5.46 correspond to CH-α of **2** (*13*), while those at δ_C/δ_H 85.2/4.62 and 71.2/4.13 correspond to CH-α/CH-α′ and CH-*γ*/CH-*γ*′ of **3**, respectively. The signals for CH-*β* of **2** and **3** (δ_C/δ_H 53.2/3.43 and 53.8/3.03, respectively) are overlapped with the very intense signal for the CH_3 of Ar-OCH_3 centered at δ_C/δ_H 55.6/3.73, and are not discernible. Moreover, the spectrum also exhibits cross-signals for CH-α of *β*-*O*-4 structure with a benzyl ether bond between C-α and C-6 of *β*-glucose unit (**8**) centered at δ_C/δ_H 81.6/4.56 (*14*, *15*), CH-6 of the glucose unit in lignin−carbohydrate complexes at δ_C/δ_H 70.0/3.52, and CH-5 of xylan backbone (**9**) at δ_C/δ_H 63.4/3.19. In addition, the cross-signals at δ_C/δ_H 73.6/3.02, 74.2/3.29, 75.1/3.41, and 77.0/3.12 correspond to oxygenated CH groups of carbohydrates. The spectrum also exhibits a cross-signal at δ_C/δ_H 102.6/4.23 corresponding to CH-1 of carbohydrates (not shown in **Figure 3A**). This indicates that either the Kraft-AQ cook had not degraded the lignin−carbohydrate complexes completely or that the lignin−carbohydrate complexes were formed in the pulping process.

Furthermore, the aromatic region of the HMQC spectrum of KRL (**Figure 3B**) shows that the KRL also contains biphenyl (5−5) structure (**4**), stilbene structure (**5**), and also 5−5 structures with a α-carbonyl and/or α-carboxylic acid group (**7**). The cross-signal centered at δ_C/δ_H 120.6/6.68 corresponds to CH-6/CH-6′ of **4**, while those at δ_C/δ_H 112.2/7.53 and δ_C/δ_H range of 126.3−127.0/7.44−7.60 correspond to CH-2 and CH-6

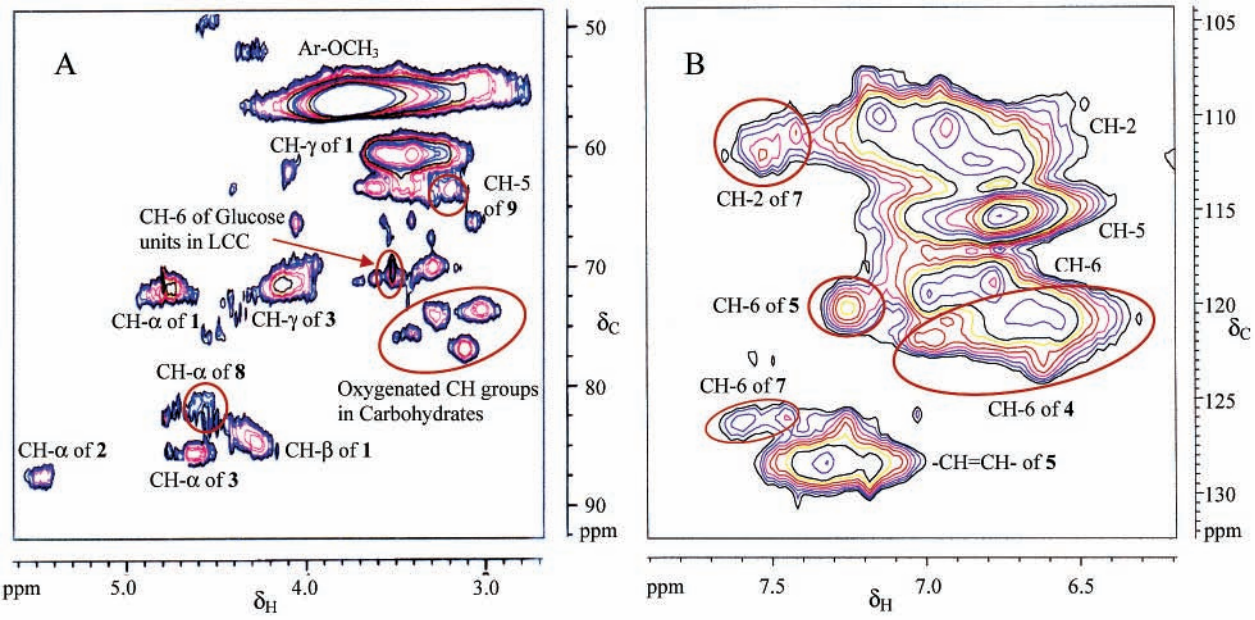

Figure 3. 2D HMQC NMR Spectra of residual lignin (KRL) prepared from the unbleached Pine Kraft-AQ pulp. (A) Oxygenated aliphatic region; (B) aromatic region. Solvent: DMSO-d_6.

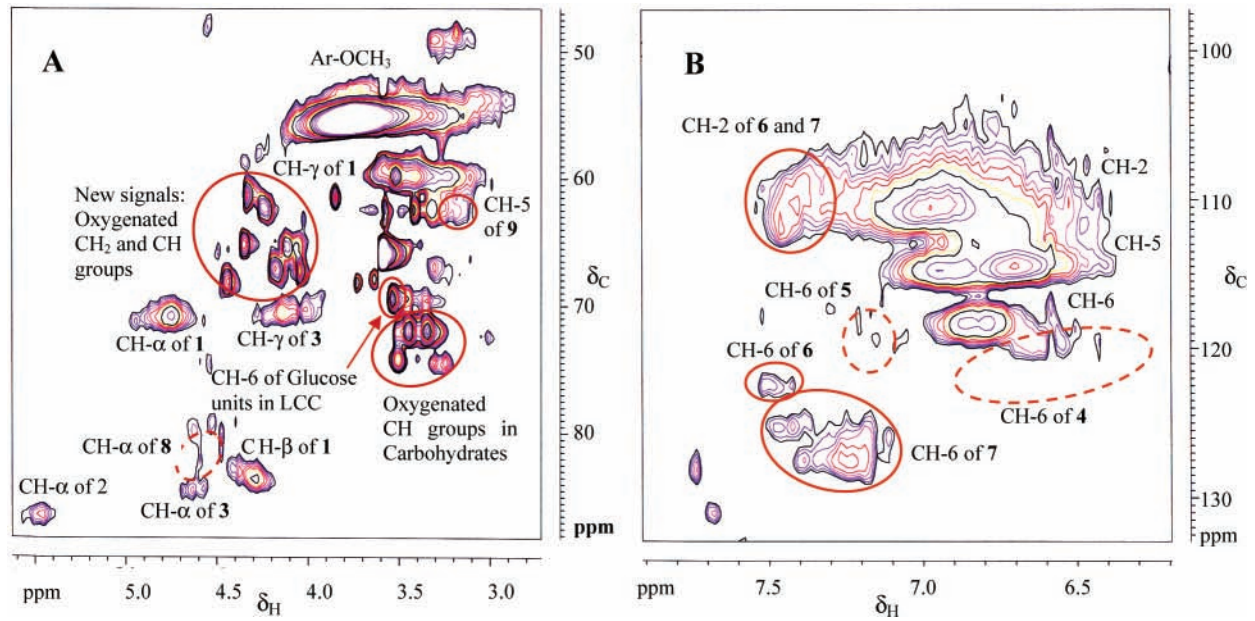

Figure 4. 2D HMQC NMR Spectra of insoluble residual lignin (ISRL-B) prepared from the bleached Pine Kraft-AQ pulp. (A) Oxygenated aliphatic region; (B) aromatic region. Solvent: DMSO-d_6.

of etherified **7**, respectively (*16*−*18*). The signals at δ_C/δ_H 120.3/7.26 and 128.4/7.32 correspond to CH-6 and -CH═CH- groups in **5**, respectively (*16*). No cross-signals corresponding to guaiacyl groups with a α-carbonyl or α-carboxylic acid group (**6**) were identified in the spectrum. It is evident that both biphenyl (**4**) and stilbene (**5**) structures are among the abundant structures in the pine Kraft-AQ residual lignin (KRL).

Structures Identified in the Insoluble Residual Lignin (ISRL-B) from the Bleached Pulp. The oxygenated aliphatic region of the 2D HMQC NMR spectrum of ISRL-B (**Figure 4A**) shows that the ISRL-B also contains *β-O*-4, *β*-5, and *β*−*β* structures (**1**, **2**, and **3**). However, the signals for these structures are somewhat less intense than the corresponding signals in the spectra of KRL. Although the spectrum does not exhibit the cross-signals for CH-α of structure **8** centered at δ_C/δ_H 81.6/4.56, it shows signals for CH-6 of glucose unit in lignin−carbohydrate complexes at δ_C/δ_H 69.5/3.52, CH-5 of xylan backbone (**9**) at δ_C/δ_H 62.6/3.21, and oxygenated CH groups of carbohydrates at δ_C/δ_H range of 72.0−74.5/3.25−3.55. This indicates that the bleaching does affect, to some degree, the degradation of the benzyl ether bonds in the structural type **8** and lignin−carbohydrate complexes. In addition, the spectrum shows new cross-signals in the δ_C/δ_H range of 61.0−67.5/4.00−4.50 corresponding to oxygenated CH_2 and CH groups. These signals must be derived mostly by way of oxidative cleavage of aromatic rings and/or oxidative degradation of LCCs and, to lesser extent, oxidative cleavage of side chain because no appreciable decrease in the intensity of signals for structures **1**, **2**, and **3** is observed in the spectrum.

In the aromatic region of the spectrum (**Figure 4B**), the cross-signals centered at δ_C/δ_H 120.6/6.68, and 120.3/7.26 are not discernible, in contrast to the corresponding spectrum of KRL.

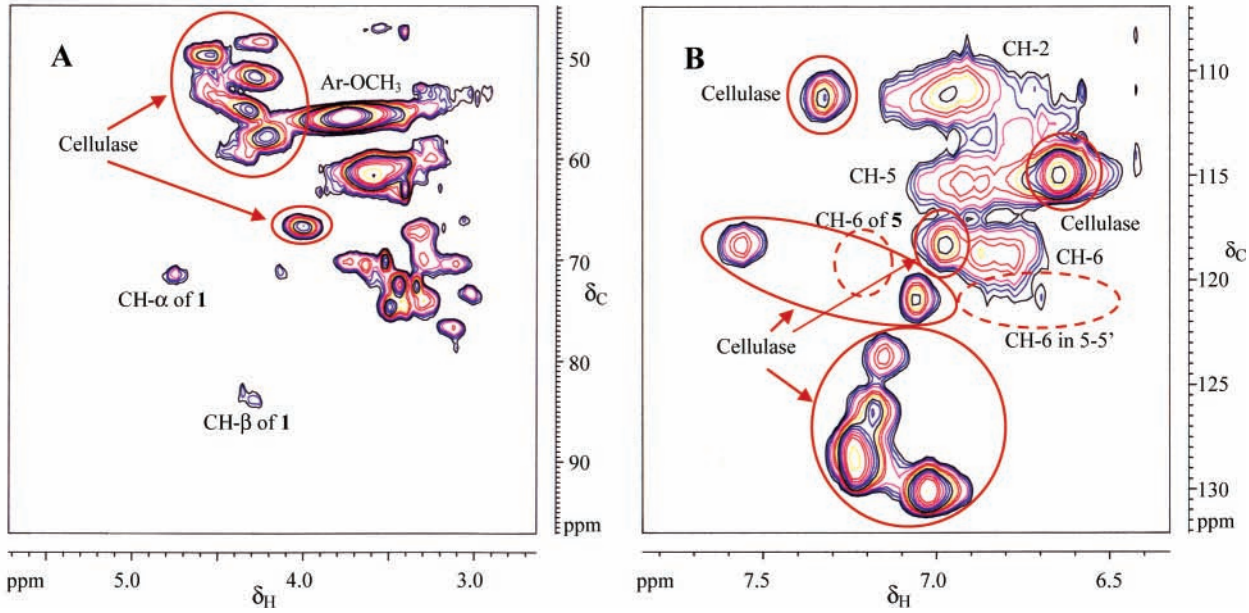

Figure 5. 2D HMQC NMR Spectra of soluble residual lignin (SRL-B) prepared from the bleached Pine Kraft-AQ pulp. (A) Oxygenated aliphatic region; (B) aromatic region. Solvent: DMSO-d_6.

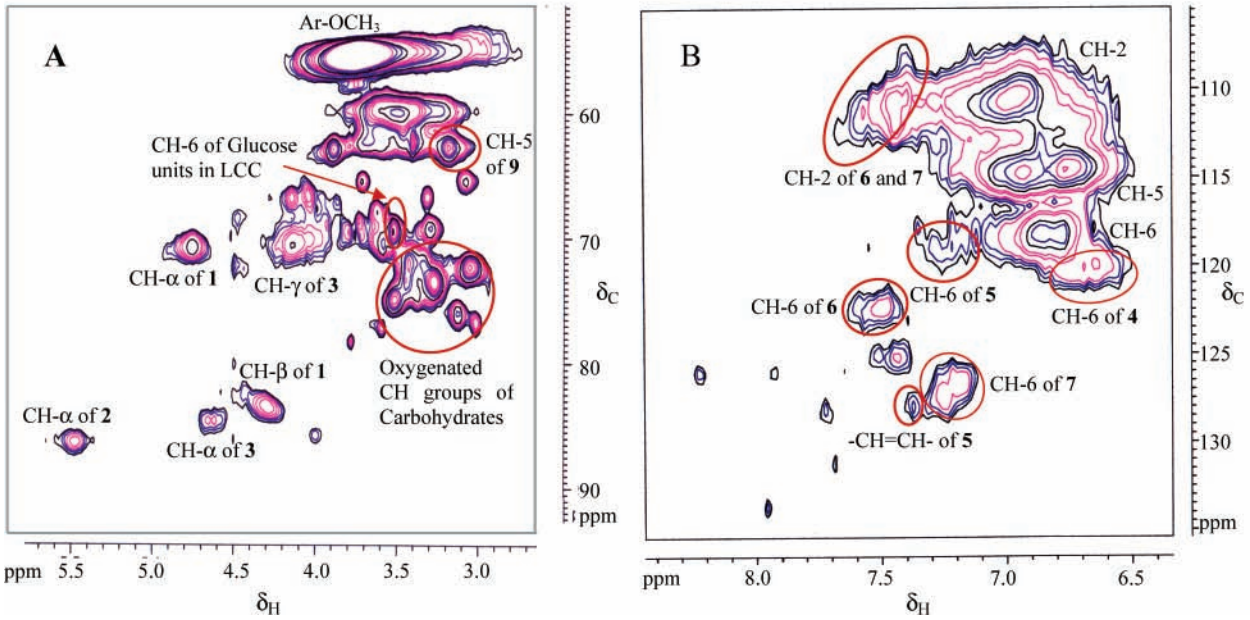

Figure 6. 2D HMQC NMR Spectra of alkaline soluble lignin (SRL) prepared from the alkaline bleaching effluent. (A) Oxygenated aliphatic region; (B) aromatic region. Solvent: DMSO-d_6.

These signals correspond to CH-6 of **4** and **5**, respectively. In addition, the intensity of signals at δ_C/δ_H range of 125−127/7.0−7.5, corresponding to etherified CH-6 of **7**, increases considerably. This cross-signal was shown to correlated to the cross-signal centered at δ_C/δ_H 112.2/7.53, corresponding to CH-2 of **7**, by the corresponding 2D HBQC spectrum (the spectrum not shown). The absence of the signal for CH-6 of **5** indicates that there is no contribution of the alkenic CH in **5**, to which these signals correspond. The spectrum also shows signals of CH-2 and CH-6 of an etherified guaiacyl structure with a α-carbonyl and/or α-carboxylic acid group (**6**). The structures **6** could be partly derived from oxidative cleavage of double bonds in the stilbene structure (**5**). Thus, it is evident that most of the 5−5 and stilbene structures (**4** and **5**) undergo oxidative cleavage of both side chains and aromatic rings in the bleaching. The -CH═CH- bond in **5** would undergo epoxidation to give an epoxide intermediate, followed by anti-Markovnikov addition of hydroperoxide anions (HOO^-) under the reaction condition, leading to oxidation cleavage of the -CH═CH- bond with formation of benzaldehyde derivatives of the type **6** (*6*). However, no signals of stilbene structures **5** were observed in the spectrum. Thus, the oxidative cleavage of the alkenic double bond in **5** cannot account for all the stilbene structures (**5**) degraded. Structures of the type **5** must also undergo oxidative cleavage of aromatic rings in addition to the oxidative cleavage of conjugated double bonds.

Structures Identified in the Soluble Residual Lignin (SRL-B) from the Bleached Pulp. As discussed previously, the SRL-B contains approximately 24% of protein contaminants derived from cellulase, according to elemental analysis. In the oxygenated regions of the spectrum (**Figure 5A**), the cross-signals at δ_C/δ_H 48.4/4.23, 49.6/4.54, 51.8/4.28, 55.2/4.31, 57.8/

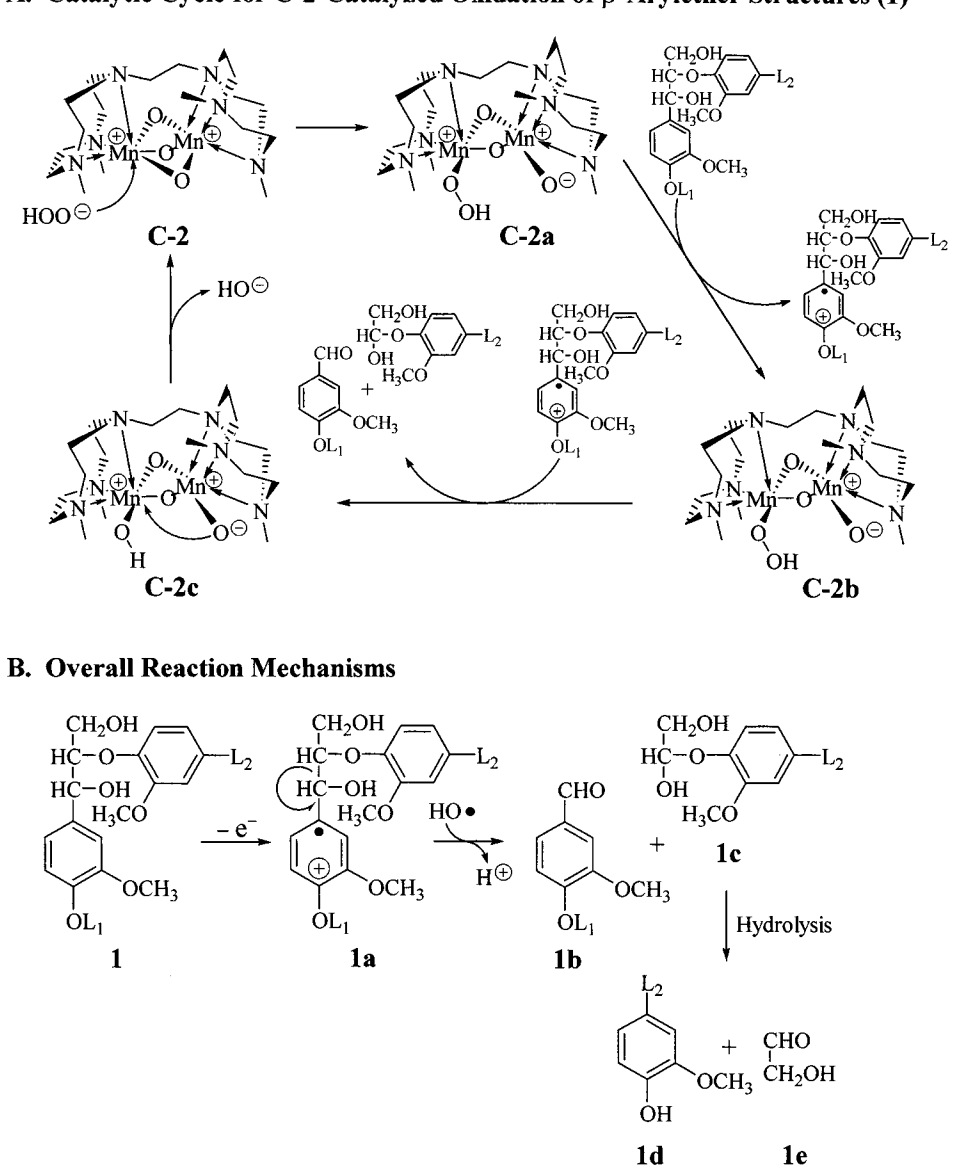

Figure 7. Catalytic cycle and reaction mechanisms for oxidative degradation of β-aryl ether (β-*O*-4) structures (**1**).

4.22, and 66.2/4.00 are from the protein contaminants. Similarly, in the aromatic region of the spectrum (**Figure 5B**), the cross-signals at δ_C/δ_H 111.4/7.33, 115.0/6.64, 118.4/6.98, 118.4/7.57, 121.0/7.06, 123.7/7.14, 126.4/7.18, 128.6/7.23, and 130.1/7.02 are also from the protein contaminants. These are verified by comparing the spectra of SRL-B with the corresponding spectra of cellulase.

Despite the contamination, the spectrum can be analyzed. In the oxygenated aliphatic region of the 2D HMQC spectrum (**Figure 5A**), very weak cross-signals corresponding to CH-α and CH-β of the β-*O*-4 structure (**1**) are discernible, but none of the signals for β-5 and $\beta-\beta$ structures (**2** and **3**) are present. In addition, no cross-signal for CH-5 of xylan backbone (**9**) and β-*O*-4 structure with a benzyl ether bond between C-α and C-6 of glucose (**8**) are detected. This could have resulted from hydrolysis of carbohydrates by cellulase, although these signals are present in the corresponding spectrum of ISRL-B (**Figure 4A**). The nature of other signals is not identified.

In the aromatic region of the spectrum (**Figure 5B**), none of cross-signals corresponding to CH-6 of 5−5 and stilbene structures (**4** and **5**) is discernible. However, signals of CH-2, CH-5, and CH-6 of guaiacyl groups are observed. The absence of signals corresponding to CH-6 of structure **5** and CH-2 in structure **7** imply that there is no contribution of -CH═CH- of **5** and CH-6 of both phenolic and etherifed **7** to the intensity of signals at δ_C/δ_H range of 123−130/7−7.3. Consequently, the signals of protein contaminants do not interfere with the analysis of the spectra in this spectral region. It is apparent, therefore, that both 5−5 and stilbene structures (**4** and **5**) undergo intensive, oxidative degradation in the bleaching in addition to the degradation of β-*O*-4, β-5, and $\beta-\beta$ structures (**1**, **2**, and **3**). As discussed previously, the stilbene structures (**5**) undergo oxidative cleavage of double bonds by way of epoxidation as well as oxidative cleavage of aromatic rings.

Structures Identified in the Alkaline Soluble Lignin (ASL) from the Bleaching Effluent. The oxygenated aliphatic region of the 2D HMQC NMR spectrum of ASL (**Figure 6A**) shows that the alkaline soluble lignin (ASL) contains rather appreciable amounts of β-*O*-4, β-5, and $\beta-\beta$ structures (**1**, **2**, and **3**). The spectrum also exhibits the signals for CH-5 of the xylan backbone (**9**) and CH-6 of glucose units in lignin−carbohydrate complexes, in addition to oxygenated CH groups of carbohydrates. Thus, it is evident that the ASL also contains considerable amounts of fragments derived from degradation of lignin−

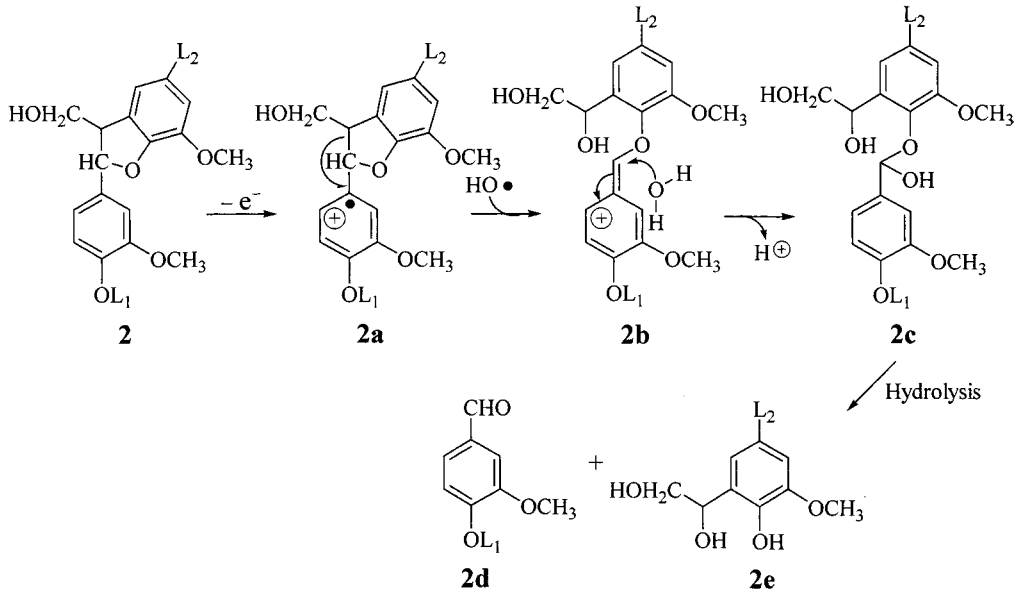

Figure 8. Overall reaction mechanisms for oxidative degradation of phenylcoumaran (β-5) structures (**2**).

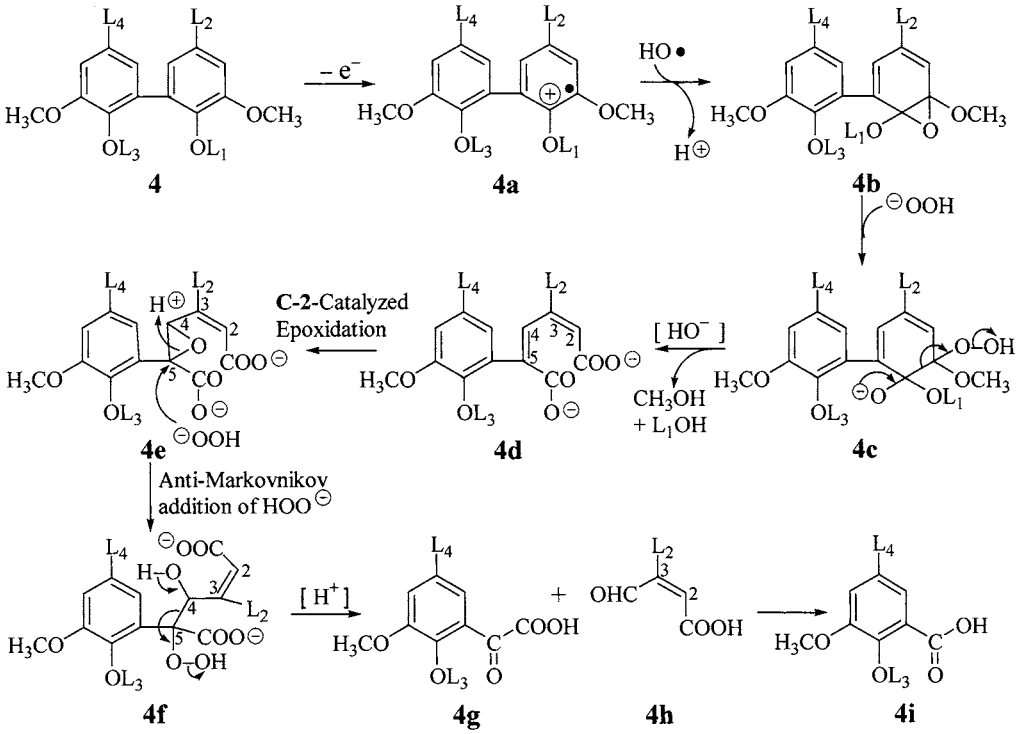

Figure 9. Overall reaction mechanisms for oxidative degradation of biphenyl (5–5) structures (**4**).

carbohydrate complexes, although it does not contain the benzyl ether bond of the type **8**.

The aromatic region of the spectrum (**Figure 6B**) exhibits only very weak cross-signals for CH-6 of 5−5 structures (**4**) and stilbene structures (**5**), in addition to a very weak signal corresponding to the -CH═CH- of **5**. However, the spectrum exhibits cross-signals corresponding to CH-2 of guaiacyl and 5−5 structures with α-carbonyl groups in structures **6** and etherified **7**. The structures **6** could be partly derived from oxidative cleavage of double bonds in stilbene structure (**5**). Signals corresponding to CH-2, CH-5, and CH-6 of guaiacyl groups are observed in the spectrum. Here again, it is evident that most of 5−5 and stilbene structures (**4** and **5**) undergo oxidative degradation.

Possible Reaction Mechanisms in the Delignification of Lignin Substructures in the Residual Lignin. In the degradation of β-*O*-4 structures (**1**) (**Figure 7**), the hydroperoxide anion (HOO^-) initially attacks one of the Mn(IV) atoms to cleave one of the three $\mu-O$ bonds. This gives the catalyst intermediate **C-2a** with one Mn(IV) atom being bonded to an -OOH group, and the other Mn(IV) atom to an $-O^-$ group. The Mn(IV)-OOH group then abstracts one electron from an aromatic ring of **1** to produce a corresponding aryl cation radial with concomitant single-electron-transfer to the $3d_{(x2-y2)}$ orbital of the $e_g(\sigma^*)$ set of Mn (IV) nucleus (*19*, *20*), which is the now the highest occupied molecular orbital (HOMO) and the oxidation state of the Mn atom is reduced to the catalyst intermediate **C-2b** with the oxidation state of Mn(III). The Mn(III) nucleus in turn

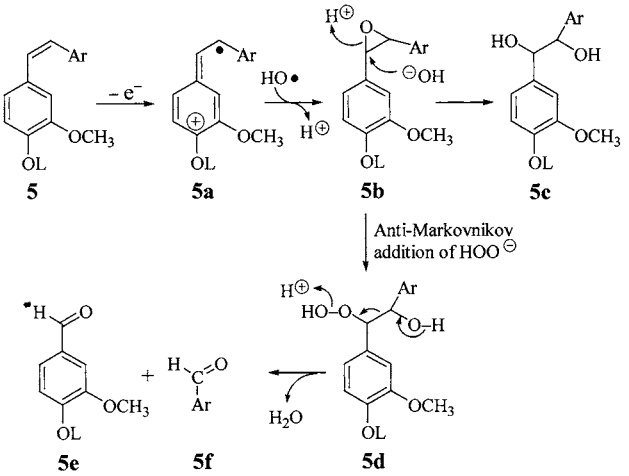

Figure 10. Overall reaction mechanisms for oxidative degradation of stilbene structures (**5**).

transfers one electron from the $e_g(\sigma^*)$ orbital to the Mn(III)-O−OH bond with concomitant release of a hydroxyl radical (HO•) that attacks C-β centered radical species resulting from $C_\alpha-C_\beta$ bond cleavage of the aryl cation radial **1a** in a concerted reaction to give fragments **1b** and **1c**, with transferring of a proton (H^+) to the catalyst intermediate **C-2b** to give the catalyst intermediate **C-2c**. Thus, the Mn(III) is oxidized back to the oxidation state of Mn(IV). The fragment **1c** then undergoes hydrolysis to produce a phenol fragment **1d** and glycolaldehyde (**1e**). Elimination of a hydroxide anion (HO^-) from the catalyst intermediate **C-2c** gives the catalyst **C-2**, completing one cycle of catalysis. The proposed catalytic cycle is consistent with the results of Gilbert et al. (*21*) and Hage et al. (*22*).

The degradation of β-5 structures (**2**) is similar to that of β-*O*-4 structures (**1**). However, as shown in **Figure 8**, a hydrolysis of intermediate **2b** is required after $C_\alpha-C_\beta$ bond cleavage of the aryl cation radial **2a** with concomitant attack of hydroxyl radical on a C-β centered radical intermediate. This gives intermediate **2c**, which undergoes hydrolysis to produce aryl aldehyde and phenol fragments **2d** and **2e**. The mechanism for degradation of $\beta-\beta$ structures (**3**) is similar with that of β-5 structures (**2**).

The degradation of 5−5 structures (**4**) involves epoxidation of aromatic rings (**Figure 9**). The aryl cation radical **4a** undergoes a concerted attack by hydroxyl radical on C-3, followed by nucleophilic attack of the resulting C−OH group on C-4 to produce epoxide intermediate **4b** and catalyst intermediate **C-2c**. The epoxide intermediate **4b** then undergoes nucleophilic attack of hydroperoxide anion (HOO^-) at C-3 in alkaline solution to give peroxyl-hemiactal intermediate **4c**. The ring cleavage between C-3 and C-4 of **4c** with concomitant base-catalyzed hydrolysis of the resulting ester groups produces muconate anion intermediate **4d** that undergoes **C-2**-catalyzed epoxidation to give 4,5-epoxy-2-hexenedioate anion intermediate **4e**. Anti-Markovnikov addition of hydroperoxide anion on C-5 of **4e**, followed by C−C bond cleavage between C-4 and C-5 of the resulting 5-hydroxyperoxyl-4-hydroxyl-2-hexenedioate anion intermediate **4f**, produces benzoyl formic acid fragment **4g** and 3-formyl-2-propenoic acid fragment **4h**. The former undergoes further oxidative decarboxylation to give benzoic acid fragment **4i**, while the latter undergoes degradation involving the double bond. Thus, 5−5 structures (**4**) are almost completely degraded, as evidenced by the fact that almost no cross-signals corresponding to CH-6/CH-6 of **4** is discernible in aromatic region of 2D HMQC spectra of ISRL-B, SRL-B, and ARL preparations. The 5−5 structures (**4**) belong to symmetry species point group C_2 (*23*). The C_2-axis passes through the bond between the two aromatic rings and bisects the angle between the two planes containing these rings. Although the structure is dissymmetric with respect to the C_2 axis, the axis bisects the structure in two parts. Because of this stereochemistry, it is conceivable that the aromatic ring of **4** undergo the oxidative cleavage more readily than those of other lignin substructures; the catalyst is trapped by the stereochemistry and electron configuration of **4**.

In the degradation of stilbene structures (**5**) (**Figure 10**), the aryl cation radical **5a** is an extended conjugated system, a C-β centered cation radical species. The attack of hydroxyl radical to the C-β, followed by nucleophilic attack of the resulting -C−OH group on C-α with concomitant transfer of a proton to the catalyst intermediate produces the diaryl-epoxide intermediate **5b** and the catalyst intermediate **C-2c**. A nucleophilic attack of hydroxide anion (HO^-) on C-α produces the 1,2-diol intermedi-

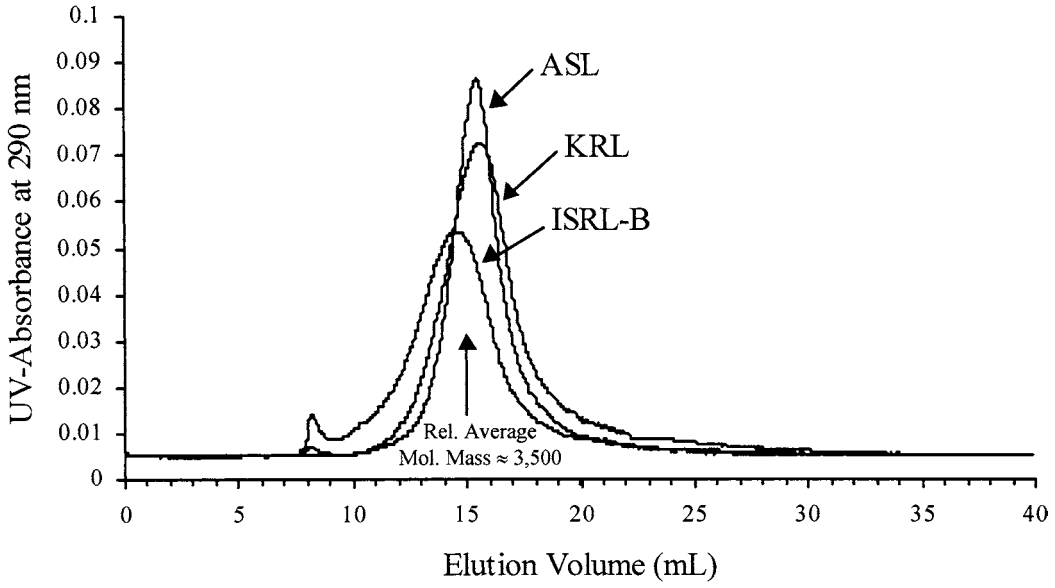

Figure 11. Molecular mass distribution of lignin preparations. KRL, residual lignin from the unbleached Pine Kraft-AQ pulp; ISRL-B, insoluble residual lignin from the bleached Pine Kraft-AQ pulp; ASL, alkaline soluble lignin from the alkaline bleaching effluent.

ate **5c** that further undergoes degradation. Moreover, an anti-Markovnikov addition of hydroperoxide anion (HOO^-) on C-α gives α-hydroperoxyl-β-hydroxyl intermediate **5d** that undergoes cleavage of the $C_\alpha-C_\beta$ bond, resulting in degradation of **5d** into aryl aldehyde fragments **5e** and **5f**. Hege et al.[22] showed that epoxidation reactions with $H_2{}^{18}O_2$ using a similar catalyst result in producing the corresponding epoxides that contained 100% ^{18}O. This suggests that H_2O_2 is the source of oxygen, not water, which is in agreement with the proposed reaction mechanism, besides the model compound experiments.

The preferential degradation of biphenyl (5−5) and stilbene structures by $Mn(IV)_2$-Me_4DTNE-catalyzed bleaching of pulps with hydrogen peroxide implied that the process is less effective in bleaching of hardwood pulps than the softwood pulp because hardwood lignin contains few biphenyl structures (*24*). In addition, the residual lignins in hardwood pulps contain much smaller amounts of stilbene structures than the residual lignins in softwood pulps (*25*). This is in good agreement with the results of Odermatt et al. (*3*).

Molecular Mass Distribution of Residual Lignin Preparations. As shown by the gel permeation chromatogram (**Figure 11**), the difference in average molecular mass among KRL, ISBRL, and ASL is far from dramatic, indicating that molecular mass is not an important factor affecting the reactivity of the residual lignin in the bleaching process. It is conceivable that other factors such as functional groups in the residual lignin play far more important roles. However, the molecular mass of KRL is lowest among the residual lignins samples examined with the major peak at an elution volume of 15.8 mL, relative average molecular mass of less than 3500 Da (= elution volume of 15.0 mL). This indicates that residual lignin in pulp undergoes delignification to lower average molecular mass fragments with concomitant condensation of the resulting phenolic fragments in the bleaching process. The GPC curve of both ISBRL and ASL shows an exclusion peak at elution volume of 8.2 mL well ahead of the major peak for ISBRL at 14.8 mL and the major peak for ASL at 15.6 mL, although the exclusion peak is very small. Even so, this indicates that the phenolic residual lignin fragments undergo dehydrogenative polymerization in the bleaching process. This in turn indicates that some radical reactions are involved in both bleaching processes in addition to nonradical reactions. There are two possible reaction mechanisms (*26*):

(i) Homolytic decomposition of hydrogen peroxide (H_2O_2) by catalytic influence of the catalyst **C-2** to produce hydroxyl radicals.

(ii) Decomposition of H_2O_2 by a dismutation reaction at alkaline pH resulting in formation of hydroxyl radicals:

$$H_2O_2 + HOO^- \rightarrow H_2O + O_2 + HO^\bullet$$

Hydroxyl radicals are very strong oxidants with a redox potential of 2.8 V. However, the dehydrogenative polymerization of phenolic fragments in the bleaching is only a lesser reaction because of very low intensity of the exclusion peaks as compared to the major peak in the GPC.

ABBREVIATIONS USED

Me_3TACN: 1,4,7-trimethyl-1,4,7-triaza-cyclononane; Me_4-DTNE: 1,2-bis(4,7-dimethyl-1,4,7-triaza-cyclonon-1-yl)ethane; HMQC: heteronuclear multiple-quantum coherence; DMSO-d_6: dimethylsulfoxide-d_6

ACKNOWLEDGMENT

The authors are also thankful to Degussa AG., Hanau, Germany, for donation of the catalyst Mn(IV)-Me_4DTNE.

LITERATURE CITED

(1) Lachenal, D.; Choundens, C.; Monzie, P. Hydrogen peroxide as delignifying agent. *Tappi* **1980**, *63*, 119−122.
(2) Alphan, C.; Andersson, E.; Andersson, S.; Hook, J. E. High-temperature peroxide bleaching of sulfate pulp. *Sven. Papperstidn.* **1977**, *80*, 480−482.
(3) Odermatt, J.; Kordsachia, O.; Patt, R.; Kühne, L.; Chen, C.-L.; Gratzl, J. S. A manganese-based catalysts for alkaline peroxide bleaching, in *Oxidative Delignification Chemistry − Fundamentals and Catalysis*; Argyropoulos, D. S., Ed.; ACS Symposium Series American Chemical Society: Washington, DC, 2001; Volume 785, Chapter 14, pp 234−254.
(4) Cui, Y.; Chen, C.-L.; Gratzl, J. S.; Patt, R. Hydrogen peroxide oxidation of lignin model compounds catalyzed by a manganese-(IV)-Me_4DTNE complex, in Proceedings of 5th European Workshop on Lignocellulosics and Pulp, Aveiro, Portugal, August 30−September 2, 1998, pp 389−392.
(5) Cui, Y., Chen, C.-L.; Gratzl, J. S.; Patt, R. A manganese(IV) complex catalyzed oxidation of lignin model compounds with hydrogen peroxide. *J. Mol. Catal. A: Chem*. **1999**, *144*, 411−417.
(6) Cui, Y.; Puthson, P.; Chen, C.-L.; Gratzl, J. S.; Kirkman, A. G. Kinetic study on delignification of Kraft-AQ pine pulp with hydrogen peroxide catalyzed by $Mn(IV)_2$-Me_4DTNE. *Holzforschung* **2000**, *54*, 413−419.
(7) Pan, X.; Lachenal, D.; Lapierre, C.; Monties, B. Structure and reactivity of spruce mechanical pulp lignins. Part III. Bleaching and photoyellowing of isolated lignin fractions. *J. Wood Chem. Technol*. **1993**, *13*, 145−165.
(8) Pan, X.; Lachenal, D.; Neirinck, V.; Robert, D. Structure and reactivity of spruce mechanical pulp lignins. Part IV. ^{13}C NMR Spectral studies of isolated lignins. *J. Wood Chem. Technol*. **1994**, *14*, 483−506.
(9) Tappi. *TAPPI Test Methods 1996−1997*; TAPPI Press: Atlanta, GA, 1996.
(10) Chang, H.-m. Isolation of lignin from pulp, in *Methods of Lignin Chemistry*; Lin, S. Y., Dence, C. W., Eds.; Springer-Verlag: Heidelberg/Berlin/New York, 1992; pp 71−74,
(11) Ralph, S. A.; Ralph, J.; Landucci, L. L. NMR Database of lignin and cell wall model compounds, available at URL http://www.dfrc.wisc.edu/software.html, 1996.
(12) Okusa, K.; Miyakoshi, T.; Chen, C.-L. Comparative studies on dehydrogenative polymerization of coniferyl alcohol by laccases and peroxidases. *Holzforschung* **1996**, *50*, 15−23.
(13) Miyakoshi, T.; Chen, C.-L. ^{13}C NMR Spectroscopic studies of phenylcoumaran and 1,2-diarylpropane type lignin model compounds. *Holzforschung* **1991**. *45*(*Suppl.*), 41−47.
(14) Freudenberg, K.; Grion, G. Beitrag zum Bildungsmechanismus des Lignins und der Lignin-Kohlenhydrat-Bindung. *Chem. Ber*. **1959**, *92*, 1355−1363.
(15) Tokimatsu, T.; Umezawa, T.; Shimada, M. Synthesis of four diastereomeric lignin carbohydrate complexes (LCC) model compounds composed of a β-*O*-4 lignin model linked to methyl β-D-glucoside. *Holzforschung* **1996**, *50*, 156−160.
(16) Kringstad, K. P.; Mörck, R. ^{13}C NMR spectra of Kraft lignins. *Holzforschung* **1983**, *37*, 237−244.
(17) Drumond, M. G.; Lemos de Morais, S. A.; Piló-Veloso, D.; Santos Cota, S. D.; Do Nascimento, E. A.; Chen, C.-L. Biphenyl type lignin model compounds: Synthesis and ^{13}C NMR substituent chemical shift additivity Rule. *Holzforschung* **1992**, *46*, 127−134.
(18) Alves, V. L.; Drumond, M. G.; Stefani, G. M.; Chen, C.-L.; Piló-Veloso, D. Synthesis of new trimeric lignin model compounds containing 5−5′ and β-*O*-4′ Substructures, and their characterization by 1D and 2D NMR techniques. *J. Braz. Chem. Soc*. **2000**, *11*, 467−473.

(19) Coulson, C. A. *Valence*, 2nd edition; Chapter X Ligand-Field Theory, Oxford University Press: Amen House, London, Great Britain, 1961; pp 276−302.
(20) Orchin, M.; Jaffé, H. H. *Symmetry, Orbitals, and Spectra*; Chapter 6 Symmetry Orbitals and bonding in transition-metal complexs, Wiley-Interscience, John Wiley & Sons: New York/London/Sydney/Toronto, 1971; pp 137−169.
(21) Gilbert, B. C., Kamp, N. W. J.; Lindsay Smith, J. R.; Oakes. J. EPR evidence of for one electron-oxidation of phenols a dimeric manganese (IV/IV) triazacyclononane complex in the presence and absence of hydrogen peroxide. *J. Chem. Soc., Perkin Trans*. **1997**, *2*, 2161−2165.
(22) Hage, R.; Iburg, J. E.; Kerschner, J.; Koek, J. H.; Lempers, L. M.; Martens, R. J.; Racheria, U. S.; Russel, S. W.; Swarthoff, T.; Robert, M.; van Vliet, P.; Warnaar, J. B.; van der Wolf, L.; Krijnen, B. Efficient manganese catalysts for low-temperature bleaching. *Nature* **1994**, *369*, 637−639.
(23) Orchin, M.; Jaffé, H. H. *Symmetry, Orbitals, and Spectra. Chapter 5 Symmetry, point group and character tables*; Wiley-Intersceince, John Wiley & Sons: New York/London/Sydney/Toronto, 1971; pp 91−136.
(24) Alder, E. Lignin Chemistry, Past, Present and Future. *Wood Sci. Technol*. **1977**, *11*, 169−218.
(25) Capanema, E. A.; Balakshin, M. Yu.; Chen, C.-L.; Gratzl, J. S.; Gracz, H. S. Studies on Kraft pulping lignins using HMQC NMR techniques. In *Proceedings of 7th Brazilian Symposium on the Chemistry of Lignins and Other Wood Components*; Belo Horizonte, MG, Brasil, September 2−5, 2001; pp 61−68.
(26) Legrini, O.; Oliveros, E.; Braun, A. M. Photochemical processes for water treatment. *Chem. Rev*. **1993**, *93*, 671−698.

Received for review September 25, 2002. Revised manuscript received December 20, 2002. Accepted December 24, 2002. This research project was supported by an USDA National Research Initiative Competitive Grand under cooperative agreement No. 98-35504-6781, for which the authors are grateful.

JF020992N